Aeronomy and Astrophysics

A ground-satellite study of the impact of solar wind variations on Pc 1 and 2 pulsations in the outer dayside magnetosphere

Mark Engebretson, *Department of Physics, Augsburg College*

Roger Arnoldy, *Space Science Center, University of New Hampshire*

Brian Anderson, *Applied Physics Laboratory, Johns Hopkins University*

The continuing deployment of Automated Geophysical Observatories (AGOs) on the Antarctic continent has made possible the establishment of an array of search coil magnetometers at geomagnetic latitudes ranging from about 66º to 85º S and geomagnetic longitudes from 15º to 40º W. These instruments provide scientists remote sensing access to dynamical processes occurring in the magnetosphere, because a variety of ultra-low-frequency (ULF) waves generated there are known to travel along magnetic field lines down toward the Earth's polar regions. In 1996 and 1997, data that we obtained from instruments at South Pole Station and at AGOs operated by the U.S. and the British Antarctic Survey, as well as from simultaneous passes of NASA's POLAR satellite.

Pc 1 and 2 waves (with frequencies from 0.1 to 5 Hz) are a common feature of the middle and outer dayside magnetosphere. It is well established that, at least for most categories, they are generated by the ion cyclotron instability, a plasma instability that requires the presence of hot, anisotropic ions that scientists believe are injected and energized on the nightside by substorm processes.

While these waves clearly have an internal source, some studies have shown that they can also be influenced by external variations in the solar wind and interplanetary magnetic field (IMF). Olson and Lee (1983), Gail (1990), and Anderson and Hamilton (1993) have noted that increases in solar wind pressure (including but not limited to sudden impulse events) often cause the waves to initiate and/or intensify. In particular, Gail (1990) showed that rather small changes in relevant plasma parameters (e.g., plasma density) in marginally stable plasmas can cause large variations in wave growth. In this study we have used the massive multistation antarctic search coil data sets from 1996 and 1997 to investigate associations between dayside Pc 1 and 2 pulsation activity and (properties of, or changes in) the solar wind and IMF.

Table 1 indicates the locations of the American and British antarctic stations used in this study. We have compared wave data from these stations against solar wind/IMF data from NASA's WIND satellite (located upstream from Earth in the solar wind) and have used this

Table 1: Locations of Ground Stations Used to Study Pc 1 and 2 Pulsations.

Location	Invariant Latitude	UT of Local Noon
South Pole Station	74º	1530
U.S. AGO P2	70º	1529
U.S. AGO P3	72º	1402
BAS AGO A81	69º	1418
BAS AGO A80	67º	1502

combined data set to group the wave events observed into four categories, three of which indicate a direct linkage to external influences:

1. Increases in solar wind density are often associated with the onset and/or intensification of pulsation activity. Sudden pressure increases initiate activity, and sudden decreases terminate it. More sustained intervals of high pressure generate sustained, large-amplitude wave events. Although we had expected to find such events, their occurrence rate was surprisingly large.
2. On other occasions, long-duration Pc 1 emissions are associated with sustained, gradual decreases in solar wind velocity. This category was not anticipated theoretically, although it is consistent with the hypothesis that plasma, moving into weaker magnetic fields, becomes more unstable to ion cyclotron wave emission.

In several cases, strong, impulsive Pc 1 activity is observed, even in the absence of upstream pressure changes. During all such events, the IMF was aligned nearly along the Sun-Earth line. Under these conditions, highly unstable, hot diamagnetic cavities are known to be generated at the bow shock (just upstream from Earth), which can cause sudden pressure changes at the magnetospheric boundary (Fairfield et al. 1990). This association is also consistent with other studies using antarctic search coil magnetometers (Arnoldy et al.1996), where sharp increases in Pc1-2 wave power were often associated with magnetic impulse events, another consequence of short-lived increases in solar wind pressure.

We found significantly fewer events than expected in the fourth category, waves that have little or no correlation — in occurrence or intensity — with external variations.

Figure 1 shows examples of both category 1 and 2 events that occurred on 8April 1996. The upper three panels of this figure use a gray scale to plot wave power as a function of frequency (vertical axis) and time (horizontal axis). Sudden, strong increases in wave power at 12:40 and 13:40 UT correlate very well with solar wind pressure variations (category 1), factoring out the 28-minute transit time of the solar wind from the WIND satellite to Earth. The sustained wave activity after 13:40 is consistent with the

sustained high level of pressure (roughly doubled) for the duration of the wave event. The more complex and somewhat weaker wave signals from 7:00 to about 11:00 UT coincide with a gradual reduction in solar wind pressure (category 2).

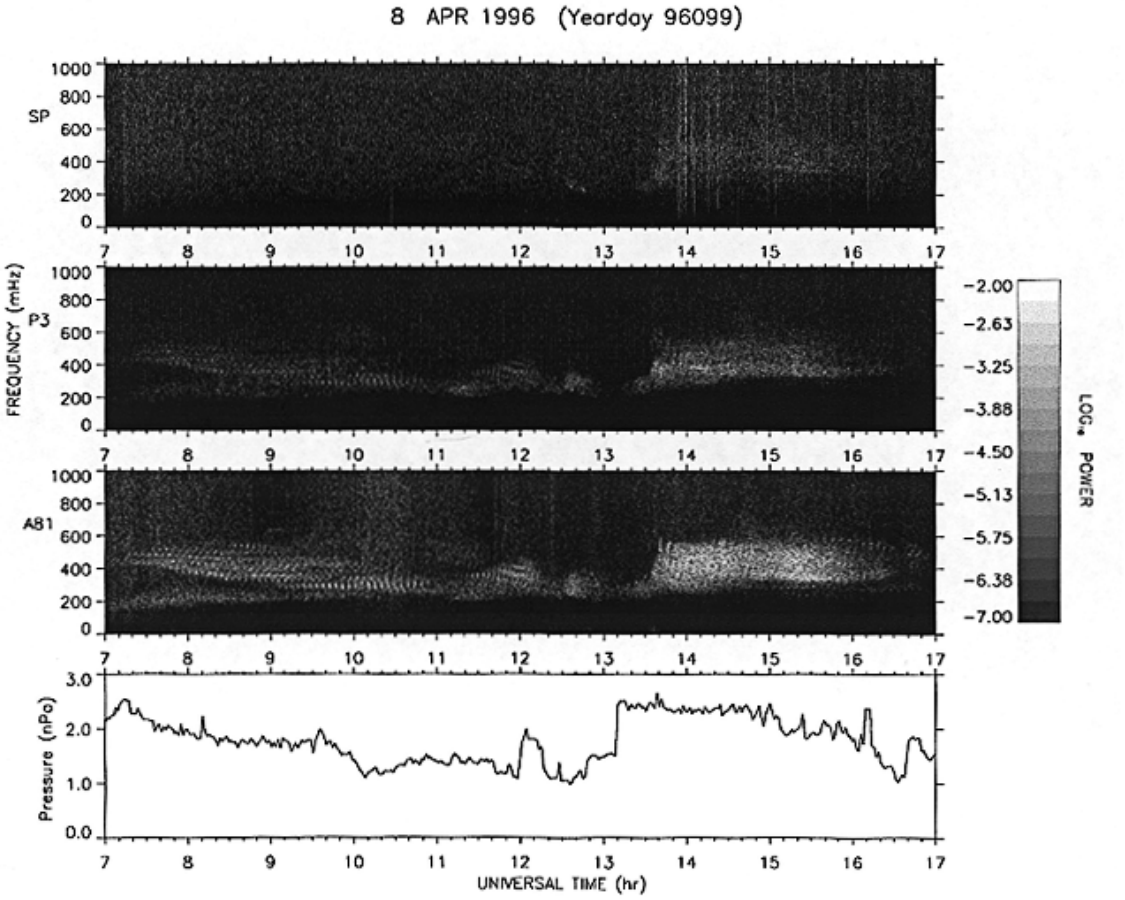

Figure 1. Plot of search coil magnetometer data and solar wind pressure (in units of nanoPascals) as a function of time from the WIND satellite from 07:00 to 17:00 UT 8 April 1996. The upper three panels are Fourier spectrograms of data from South Pole Station, AGO P3, and AGO A81, respectively. For these panels, the vertical axis corresponds to wave frequency; the gray scale shows the wave intensity.

Figure 2 compares the signatures of the last wave event on 8 April from AGO P3 with those obtained by the POLAR satellite as it passed through the dayside magnetosphere (about 30º E of P3. POLAR only observed waves near 14:25 UT, the time that the satellite crossed magnetic field lines mapping to very near the latitude of P3. The lower part of this figure shows details of the power as a function of frequency during the interval 14:22 - 14:30 UT. The good (but not perfect) agreement in frequency spectrum suggests that the waves are generated on magnetic field lines over a limited range of latitudes near that of P3. The agreement in location and timing given in this event is typical of that found in our 2-year data set.

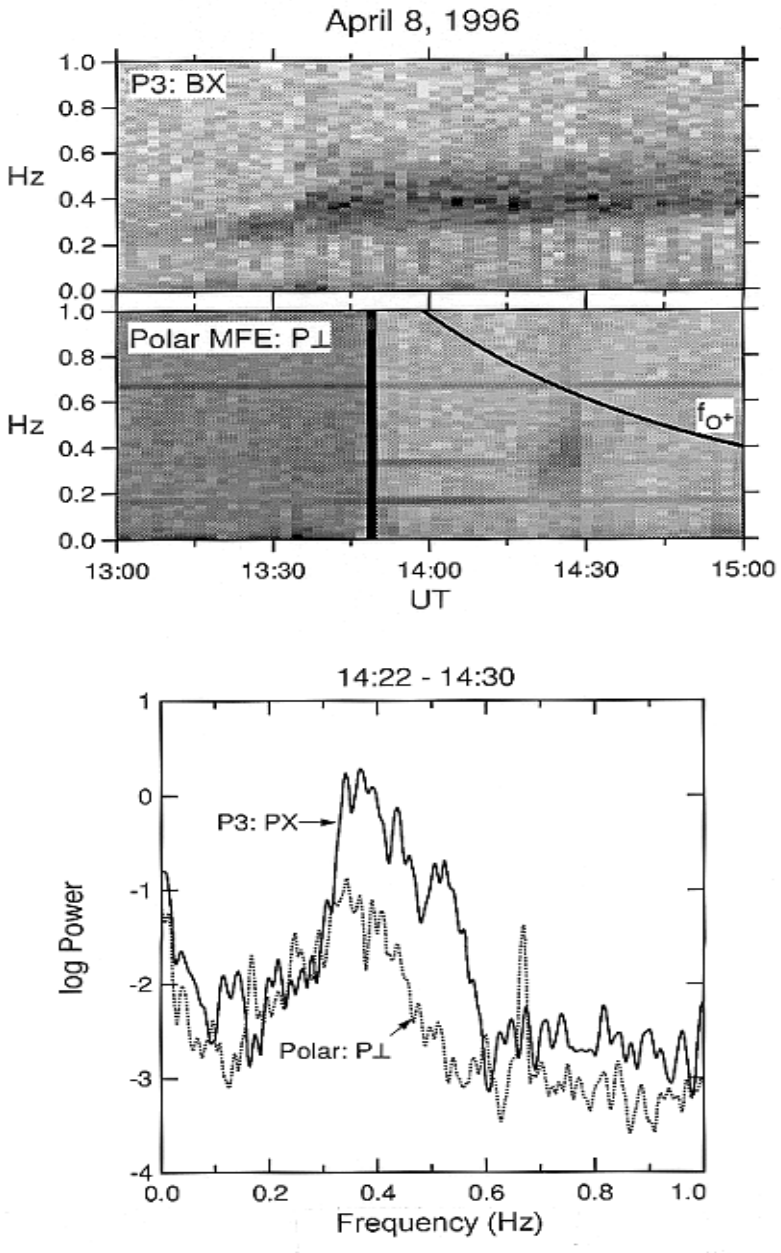

Figure 2. The Pc 1 event of 8 April 1996 as seen from AGO P3 and the POLAR satellite. The upper panel shows spectrograms from 13:00 to 15:00 UT. The lower panel shows line spectra for the period 14:22-14:30 UT, when waves were observed both in space and on the ground.

Table 2 groups the results our statistical survey by year and event type. For both years, the breakdown is very similar: roughly half the wave events (category 1) are directly associated with increases in external pressure. The fraction of events not clearly associated with some kind of external variation (category 4) is considerably lower than we had expected on the basis of our current understanding.

Table 2: Daily occurrences of Pc 1 and 2 waves as a function of solar wind/IMF conditions or variations

Category	Pressure Up	Pressure Down	Radial IMF	No correlation or ?
1996	47%	9%	12%	31%
1997	51%	11%	7%	31%

Because this last category still comprised roughly one third of the wave events, we looked for a temporal correlation with magnetic storms, comparing Pc 1and 2 event occurrence to the Dst geomagnetic activity index. But, there was little correlation between even this category of Pc 1 and 2 waves and intervals of negative Dst, which are associated with geomagnetic storms or their recovery phases.

These several observations suggest that the dayside magnetosphere is frequently marginally unstable to ion cyclotron wave emission, regardless of the temporal proximity to nightside particle injections, and that field compressions are the dominant source of the free energy that causes and sustains these emissions.

We thank Hiroshi Fukunishi of Tohoku University, Sendai, Japan, for his leadership in developing the search coil magnetometers deployed at the U.S. AGOs, and Jennifer Posch, Ryan Cobian, and Matthew Klatt for their help in data analysis. This research was supported by National Science Foundation grants OPP 93-15750, OPP 95-29177, and OPP 96-13683.

References

Anderson, B. J., and D. G. Hamilton. 1993. Electromagnetic ion cyclotron waves stimulated by modest magnetospheric compressions. *Journal of Geophysical Research*, 98, 11369-11382.

Arnoldy, R. L., M. J. Engebretson, J. L. Alford, R. E. Erlandson, and B. J. Anderson. 1996. Magnetic implulse events and associated Pc 1 bursts at dayside high latitudes., 101, *Journal of Geophysical Research*, 7793-7799.

Fairfield, D. H., W. Baumjohann, G. Paschmann, H. Luehr, and D. G. Sibeck. 1990. Upstream pressure variations associated with the bow shock and their effects on the magnetosphere. *Journal of Geophysical Research*, 95, 3773-3786.

Gail, W. B. 1990. Theory of electromagnetic cyclotron wave growth in a time- varying magnetoplasma. *Journal of Geophysical Research*, 95, 19089-19097.

Olson, J. V., and L. C. Lee. 1983. Pc 1 wave generation by sudden impulses. *Planetary and Space Science*, 31, 295-302.

WHOOPS: An improved rooftop optical shelter

K. C. Clark and G. Hernandez, *Graduate Program in Geophysics, University of Washington, Seattle, Washington*

We report here a new kind of housing for a rooftop, sky-scanning mirror assembly, which performed better throughout its first winter of use than any of our earlier dome designs of the past decade, at the South Pole. Our Fabry-Perot spectrometer successively views with this mirror the sky at the zenith and eight azimuthal directions of 30º elevation. Through this viewing mechanism, we measure the waves of wind and temperature at mesospheric heights by performing Doppler interferometry on the naturally occurring emissions of the atmosphere. These repeated delicate measurements require reliably clear viewing through windows and a sheltered warm interior environment for the moving mirror.

Although in earlier years a separated pair of thin (3-6 mm) acrylic domes (Clark et al. 1994) with dry and ultrapure nitrogen circulating in their separation gap has usually kept the view free of condensation, a new simpler, surer solution to the previous occasional fogging has been established. We now suspect that the release of water absorbed by the acrylic itself may likely have been the recurrent source of condensable water vapor in the gap between hot and cold dome surfaces. By manufacturer's report, an acrylic piece can itself absorb water up to 1 to 2 percent of its own weight. Much smaller amounts captive in our former domes could have supplied some of the condensation that occurred in our double-paned separation gap. This may explain earlier occasions of our inability to stay entirely free of all fogging of the inner surface of the outer dome under South Pole temperature extremes.

We describe here a new design approach, which proved itself over the 1998 winter. It completely eliminates the air gap between the domes, and thereby the condensable humidity, by using single thick walls of acrylic to form an octagonal flat-roofed viewing housing for the same mirrors. Its thickness of 1.6 cm for the single walls and roof worked well, and 2.0 cm or thicker could be even more effective.

Called the WHOOPS (What a Heavy Octagonal Optical Portal System) by its on-site technicians, it simply has removed any gap (as between former domes) between the outdoors and indoors where moisture droplets could possibly condense. The single much thicker plates not only deny a cold surface for condensation but also keep the heat conduction low and all mirrors, adequately warm with no increase in heating power. Heated air is blown against the interior wall faces from a low single-ring manifold of 5-cm-pipe with 90 outward-slanting, uniformly spaced jet holes of about 0.25 cm. diameter. Finally, the cooler interior air leaves via a floor port, for closed-path heating and return.

The sheltered interior mirror assembly must receive a wide beam (10 cm) of parallel sky light from each chosen direction. These slanting directions are preserved, in spite of refraction, by the parallelism of inner and outer faces of each smooth wall. The

transverse displacements of sky light at 30º elevation are easily accommodated by the ample sidewall areas.

The material chosen is colorless Acrylite GP, a standard type of cell-cast sheet with a 10-year manufacturer's warranty on light transmission. No special ultraviolet transparency is required for our use. The edges of vertical walls are bevelled radially to fit flat together at each octagon comer. The total window assembly rests loosely in shallow horizontal grooves in the separate acrylic roof and floor sections. All edges fit generously enough to minimize possible thermal strains and are filled with DC-3140 silicone rubber. The assembly is held together rigidly by vertical stainless steel tension rods through roof and floor outside each octagon corner. These rods have brazed T-heads fitting into external short slots in the acrylic floor bottom and have upper ends extending beyond external threaded assembly nuts and compression lock washers on the roof. A linear bead of DC-3140 silicone along the outer edges of windows assures a good weather seal.

A sketch of the final WHOOPS assembly is shown in the figure. The surface area for heat conduction is 1.11 m^2 and the mass is about 26 kg. It can be lifted edgewise through the 76-cm-square hatchway for installation on the roof of the Skylab building.

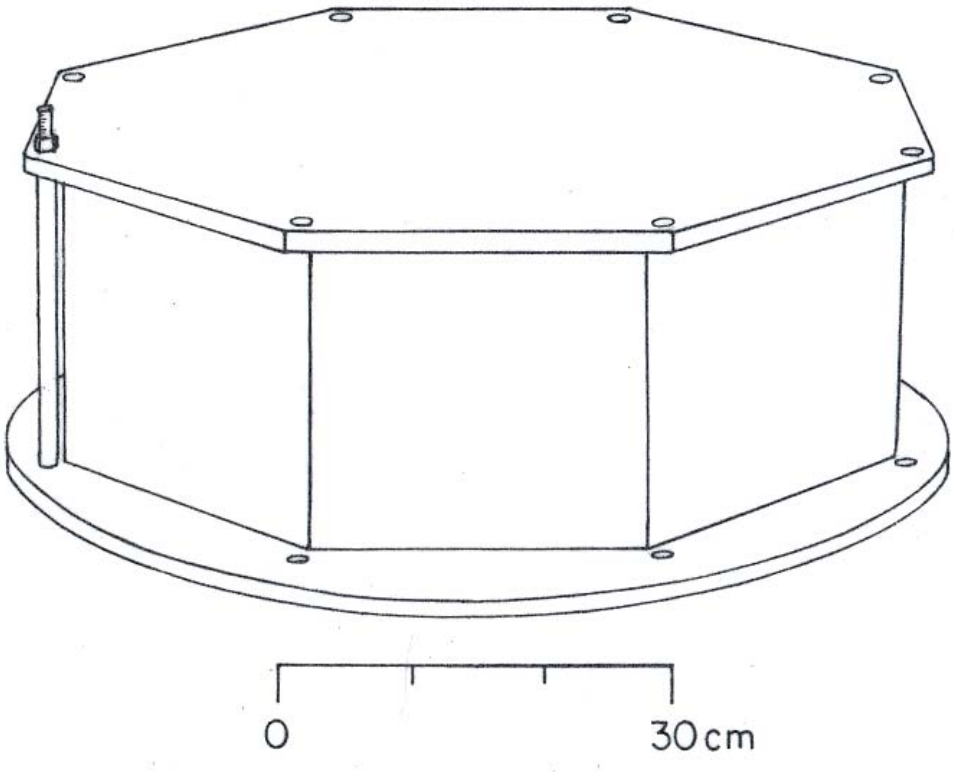

Drawing of assembled WHOOPS. One tension rod is shown.

This first constructed WHOOPS has given good mechanical operation and clear viewing without demanding more heat power than the 400 watts of the previous double dome assembly. Slightly thicker walls would further reduce heat loss for the same functioning, although the overall size and weight are close limitations. Through the first winter, the horizontal roof showed negligible tendency to collect blowing snow. In summer, a plywood box-like cover is placed over the WHOOPS, as was done for the previous domes, to avoid abrasion, contamination, and yellowing by sunlight.

An external roof layer of 5-cm blue styrofoarn was added for the 1999 winter season to evaluate its effectiveness in further reducing heat loss. It covers most of the roof except for the edge segment through which zenith measurements are made. The removable styrofoam insulation layer is fastened by extension bolts connecting to six of the existing corner tension rods. It is expected not to produce accumulation of blowing snow at the unprotected zenith viewing position near the edge.

The set and scaled housing described above showed no differential thermal expansion difficulties over the first year of use and, in fact, no problems of any kind. This demonstrated use of single very thick acrylic windows could be an exemplary and practical alternative for fogged standard thermopane windows at other South Pole installations.

This work was supported in part by National Science Foundation grant OPP 96-15157.

References

Clark, K. C., G. Hernandez, W. J. Schulz and R. W. Smith. 1994. Optical all-sky viewing double-dome for South Pole, *Antarctic Journal of the U. S.,* 28, 5.

Broad diffuse source for optical intensity calibration

K.C. Clark and G. Hernandez, *Graduate Program in Geophysics, University of Washington, Seattle, Washington*

It is necessary to monitor the constancy of gain for each detector head (consisting of dichroic mirrors, interference filters, collimating optics, and photomultiplier tube) operating in our double detection systems for Fabry-Perot spectrometers. We require a constant and uniform white-light source to substitute in front of the detector head in the 3.6-cm diameter optical beam. It must fit entirely into a narrow 1.8-cm gap without disturbing any optical adjustments on either side. The novel source described here has been very useful. It is completely housed in a transverse metal slide of dimensions equal to those of a removable filter holder, fitting the same 6.3 by 1.8-cm slot without affecting the alignments of other optical components. The principles and description of this wide, thin uniformly bright light source are presented here.

The source makes use of scattered light from an ideal Lambertian surface. An ideal diffuse (Lambertian) rough, thick white scattering surface returns all light striking it—each area element S sending out various intensities per solid angle that are a maximum M along the surface normal and M cos$\ominus$ in other directions. Since the projected surface area of S is S cosa, this element appears equally bright in all directions of view. The surface element S and all the extended broad surface of which it is a part are curved to form a concave partial sphere of radius R, all of which is illuminated by the entire concave surface.

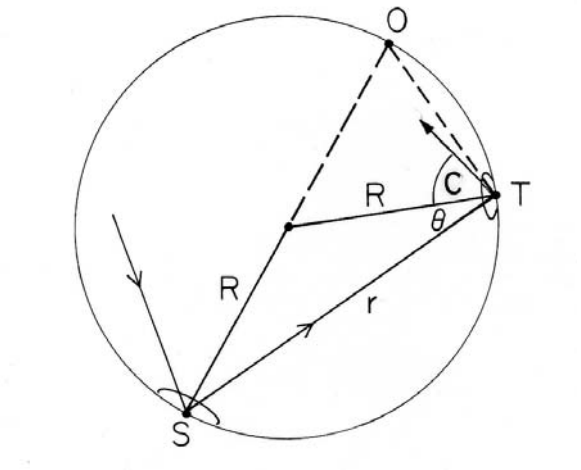

Figure 1. Scattering geometry. Hemisphere angle* STO *always is 90º.

Because of $M \cos\ominus$, each elemental receiving area T of the surface receives from a given S the same amount of light flux through its cone, as this area T is proportional not only to the square of the direct ray path r but also to the secant of the angle $\ominus$ between the ray and the surface normal to T. Figure 1 illustrates these statements, showing the circle section that contains S, T, and the point O opposite to S. Angle STO is 90º in all cases, as it subtends half a circle. Therefore, we have

$$r = 2\,R\cos\ominus\,. \qquad 1)$$

The solid angle Ω of each elemental cone from S bounding any T is

$$\Omega = T\cos\ominus / r^{2} \qquad 2)$$

Carried in it from S is the flux F given by

$$F = M\,\Omega\cos\ominus = M\,T\cos^{2}\ominus / r^{2} \qquad 3)$$

But we see from geometry that $r^{2} = 4\,R^{2}\cos^{2}\ominus$. The flux per surface receiving area reaching T from S is therefore simply

$$F / T = M / 4\,R^{2} \qquad 4)$$

The fact that this incident flux per receiving area is the same, regardless of source position angle $\ominus$ over the partial spherical surface, provides the uniformity of our viewed brightness across the entire source breadth. The flux from S is rescattered by the Lambertian surface T. Part of this re-scattering hits elsewhere on the surface for re-use. Part escapes, some contributing to the flux received by an external person or detector situated at an angle C relative to the normal at T. This received flux has come by Lambertian scattering from T in proportion to $\cos C$, as well as from the projected emitting area $T\cos C$. The detector's received flux per solid angle subtended by the scattering source T, therefore, does not vary with either T or C. Since this fact does not depend on where T is situated across the spherically curved Lambertian surface, the whole source appears to the detector to be uniformly bright.

This same reasoning also applies for all subsequent scatterings by the total area onto itself and away. Given the close approximation of the practical surface to a perfect Lambertian scatterer, we conclude that any large or small piece of such a spherically curved surface, first illuminated by scattering from an initial bright portion of the same surface, will appear uniformly bright. However, if that initial area element S is illuminated not only by local scattering but first by an independent external source, then that S has greater brightness than the rest and must be excluded from the external view of uniformity. This exclusion is usually not difficult to arrange.

It has proved easy to obtain adequate concave diffusing surfaces simply by making white plaster casts of convenient convex spherical lens faces of maximum widths from 2.5 to 20 cm. For our current needs, the diffuse Lambertian character of this white plaster surface was found to be quite satisfactory without a special coating of barium sulphate paint. The present device uses a 4.3-cm plaster square that is 1.2 cm thick and carries the cast of a lens face having 4.6 cm radius of curvature. Its extreme corner peaks (not used) are slightly relieved to keep a workable center thickness of the plaster when the back of the cast is flattened and glued to a mounting plate. Figure 2 gives line drawings in perspective showing the components of this working source.

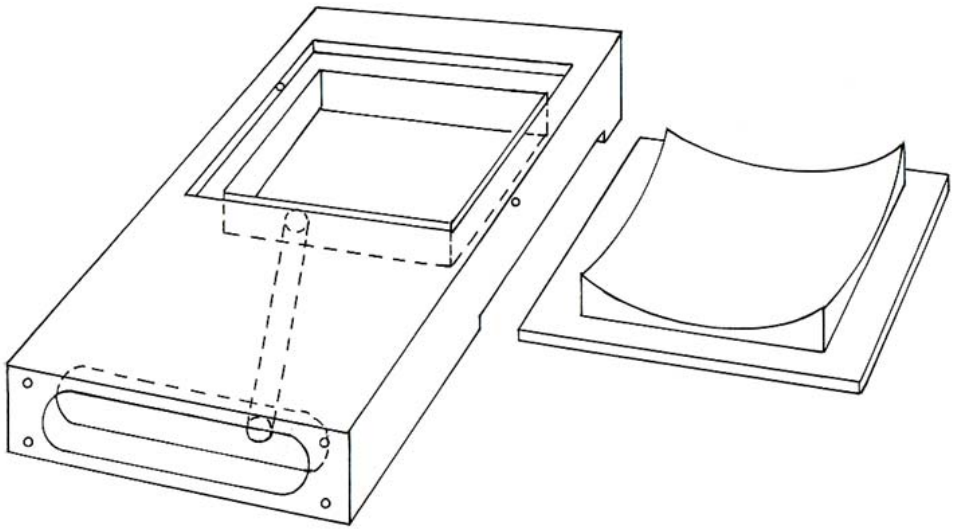

Figure 2. Configuration of source and holder.

Illumination comes from a standard miniature incandescent lamp (#222) powered conservatively by a constant current source. A slanting tunnel contains a lens and two diaphragms; they project a small bright image spot to the far corner of the square section of the curved scattering surface. This source spot is obscured from external view by a 0.6-cm black paper piece which is glued above it but below any external sliding contact. When viewed in a dark room, the remaining entire insertion source area illuminated by scattering appears remarkably uniform. Results of a photometric scan along a face diameter are shown in figure 3 and confirm the above predictions. The present configuration provides an ample width of beam for our instrument use, as our collimated beams there are 3.43 cm wide and in fact circular.

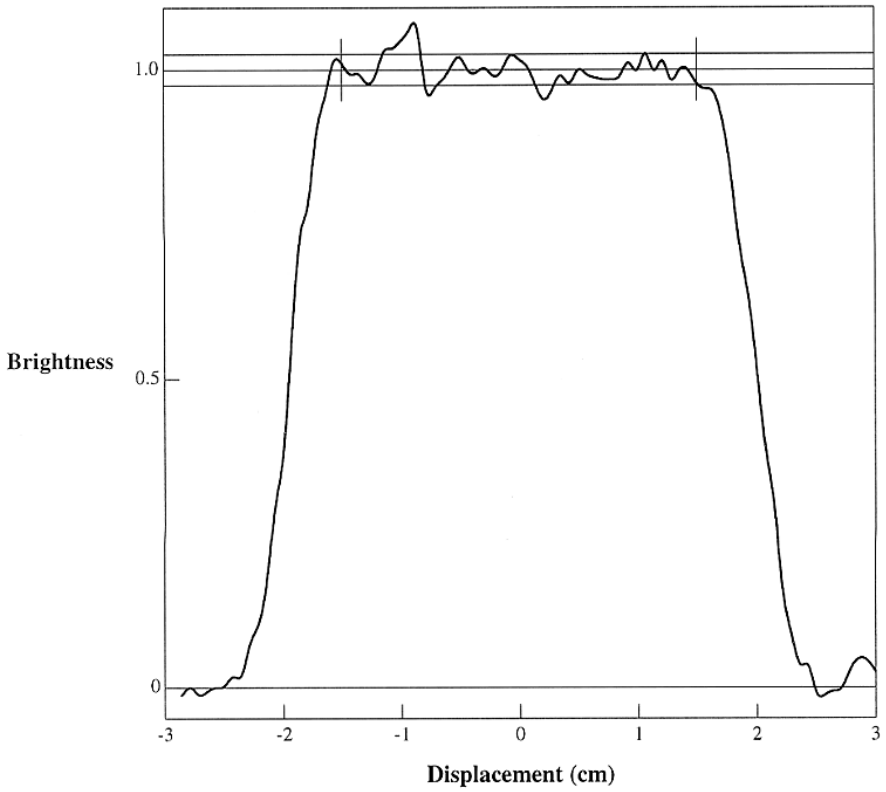

Figure* 3. *Relative brightness across diameter. The experimentally found ±2.5% root-mean-square variation (in the region encompassed by the two vertical bars) is indicated.

The simple concave diffuse scattering geometry exploited in this novel device is notable for its basic simplicity, its non-invasive and repeatable performance in sensitive optical measurements, and its scalability to much larger dimensions to match new applications. The general principles are long a part of optics tradition, back certainly as far as the integrating spheres of Ulbricht (1900) and as recently as the partial sphere photometry of Young et al. (1976). The present report contributes a particularly opportune and practical application of this photometric geometry to environmentally rigorous, yet precise, field optical instrumentation.

This investigation was partially supported by OPP 93-0273.

References

Ulbricht, R., 1900. Die bestimmung der mittleren raumlichen lichtintensitat durch nur eine messung. *Elektrotechnische Zeitschr.* 21, 595-597.

Young, E. R., R. B. Bennett, and T. L. Houk, 1976. Diffuse low brightness calibration using a partial photometric sphere. *Trans. Amer. Geophys. Union (EOS), 5 7, 3 11.*